IChemE

0960–3085/00/$10.00+0.00

Trans IChemE, Vol 78, Part C, March 2000

ROLE OF THERMO-RHEOLOGICAL BEHAVIOUR IN SIMULATION OF CONTINUOUS STERILIZATION OF A STARCH DISPERSION

H-J. LIAO, M.A. RAO, and A.K. DATTA*

Department of Food Science and Technology, Cornell University, USA
**Department of Agricultural and Biological Engineering, Cornell University, USA*

Continuous sterilization of a starch-containing fluid food in a tubular heat exchanger with heating and cooling sections was simulated numerically. Experimentally determined thermo-rheological (TR) behaviour during gelatinization of a starch dispersion was used for the fluid flowing in the heating section and a shear-thinning model combined with the Arrhenius equation was used for the cooling section. The observed plug-flow profile in the heating section was caused by gelatinization of the starch-containing fluid food that, in turn, affected the accumulated lethality and thiamine retention. Using smaller diameter tubes resulted in better nutrient quality (higher thiamine retention). Higher thiamine retention also resulted from lower heating wall temperature, even though a longer heating tube was required to achieve the required sterility. Higher volumetric flow rate resulted in longer length of the heating section in order to achieve the sterility of the product but the nutrient retention was almost unchanged.

Keywords: continuous sterilization; starch dispersion; thermorheology; nutrient retention

INTRODUCTION

In continuous flow (CF) sterilization, the fluid food product and containers are sterilized separately, and brought together in an aseptic environment for packaging (aseptic processing). One advantage of CF sterilization over conventional canning (batch sterilization) is that the product quality can be improved (e.g. higher nutrient retention) because the food can be heated more rapidly due to flow and higher sterilization temperatures[1].

In earlier heat transfer studies applicable to continuous flow sterilization[2,3], where a fluid was heated at a constant wall temperature, the physical properties of the fluid were assumed to be independent of temperature. Two expressions in thermo-rheology, isoviscous and non-isoviscous flow, are noteworthy; the former is defined as the flow of a fluid with a temperature-independent rheological behaviour and the latter as flow of a fluid with temperature-dependent rheological behaviour. However, because of variation in temperature in the radial and axial directions, the physical properties of the fluids, especially the rheological properties, may vary significantly. Isoviscous flow appears to be of relatively minimal value in practical applications. Christiansen and Craig[4] combined the effect of temperature described by the Arrhenius equation with the power law equation to characterize the rheological properties of the fluid being heated as a function of both temperature and shear:

$$\sigma = K_0\left(\dot{\gamma}\exp\frac{E_a}{RT}\right)^n \tag{1}$$

Simpson and Williams[1] studied the inactivation of bacterial spores at the centreline of a tubular sterilizer assuming it to be equivalent to a batch sterilization process carried out at 121°C for 2.45 min, so that log $(c/c_i) = -11.5$. The most important effect of the non-isothermal nature of a CF process is that radial temperature gradients cause radial viscosity gradients that in turn lead to considerable distortion of the velocity profiles. For sterilization of low-acid shear-thinning fluids, Simpson and Williams[1] suggested a total dimensionless length (ζ) of 1.2 with 0.8 for the heating section and the remaining 0.4 for the cooling section:

$$\zeta = z\alpha/R^2u_{avg} \tag{2}$$

Based on numerical calculations, the variation in the recommended dimensionless length was found to be within ±2% for $0.3 \leq n \leq 1.0$ and $-4 < \psi < 4$, and the strength of coupling of the momentum and energy transport equations was characterized by the equation:

$$\psi = \frac{E_a}{R}\left(\frac{1}{T_0} - \frac{1}{T_w}\right) \tag{3}$$

The holding section was not considered to minimize thermal destruction of nutrients.

Kumar and Bhattacharaya[5] simulated aseptic processing of a non-Newtonian fluid with temperature dependent and shear thinning viscosity in a tubular heat exchanger; they demonstrated that a lower wall temperature and smaller diameter tube can improve product. Jung and Fryer[6] studied optimization of the quality of Newtonian and non-New-

tonian foods under non-isoviscous conditions using the CFD package FIDAP.

In many food products, starch is used as a thickening agent. Although many foods are subjected to thermal treatments prior to sterilization, often the treatments are not sufficient to achieve complete starch gelatinization. As a result, broken heating curves are encountered during batch sterilization of many starch containing foods[7]. The viscosity of a fluid containing starch increases first with temperature during thermal processing because of the amylose released, and swelling of the starch granules after the initial temperature of gelatinization has been reached. After the dispersion has attained its maximum viscosity, the granules begin to rupture so that the viscosity decreases with temperature[8,9]. Therefore the viscosity model obtained by combining the power law model with the Arrhenius equation fails to describe the rheological behavior of starch-containing fluids during the course of gelatinization. Yang and Rao[10] proposed a thermo-rheological (TR) model for a starch-containing fluid food that was based on dynamic rheological data obtained as a function of temperature at several oscillatory frequencies. Using temperature sweep tests, they obtained a set of complex viscosity vs temperature curves at different oscillatory frequencies that were superposed by translation along the viscosity coordinate with a shift factor $(\omega/\omega_r)^{\beta}$ resulting in a master curve.

$$\eta^*_R = \eta^* \left(\frac{\omega}{\omega_r}\right)^{\beta} \tag{4}$$

The objective of this study was to study the non-isothermal sterilization of a 4% waxy rice starch dispersion in laminar tube flow for different flow rates, heating wall temperatures, and tube diameters using experimentally determined TR behaviour. Finite element-based solutions were obtained to the coupled governing momentum and heat transport equations of the problem formulated. The velocity and temperature profiles in the tube were used to predict the cumulative lethality on the slowest heating zone (SHZ) and the mean bulk nutrient retention at the end of heat transfer section. The results should be useful for optimization of sterilization process parameters for starch containing foods.

PROBLEM FORMULATION

Model of Non-Isothermal Laminar Tube Flow

A straight tubular heat exchanger, similar to that studied by Simpson and Williams[1] (see Figure 1), into which the starch-containing fluid food was pumped at an initial temperature $T_0 = 25°C$, with a fully developed velocity profile at the entrance of the tube, was considered. The heating section was held at a constant wall temperature (T_w) and its length was terminated when the accumulated lethality value on the centreline reached 5.0 min, which was close to the practical thermal process design criteria in the food industry. At the end of the heating section, the hot fluid food was cooled immediately in a cooling section with an arbitrarily selected wall temperature of 25°C; the length of the cooling section was assumed to be 10 m.

The following assumptions were made in the analyses:

1) the flow was at a steady state;
2) the flow was rectilinear and axisymmetric about the centre line which made the problem two dimensional instead of three dimensional;
3) the fluid thermal conductivity, specific heat, and density were independent of temperature and pressure;
4) at the entrance to the heat transfer section, the flow had a uniform temperature and was fully developed;
5) thermal energy generation in the fluid by viscous dissipation or by reaction was negligible;
6) natural convection effects were negligible;
7) the fluid was considered to be homogeneous; and
8) there was no slip at the wall.

The governing conservation equations and the boundary conditions in non-isothermal laminar tube flow are as follows:

- equation of continuity:

$$\frac{\partial u}{\partial z} + \frac{1}{r}\frac{\partial}{\partial r}(r\nu) = 0 \tag{5}$$

- equation of motion:

$$\rho\left(u\frac{\partial u}{\partial z} + \nu\frac{\partial u}{\partial r}\right) = \frac{1}{r}\frac{\partial}{\partial r}(r\sigma_{rz}) + \frac{\partial \sigma_{zz}}{\partial z} \tag{6}$$

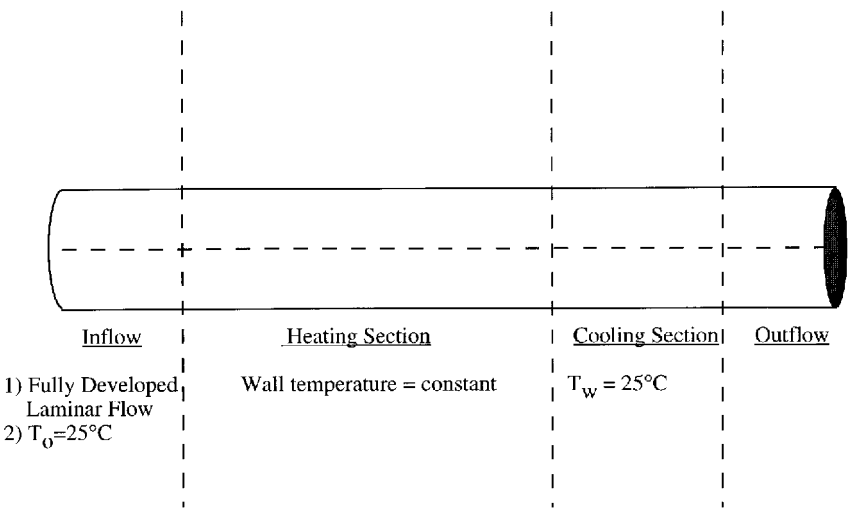

Figure 1. Continuous tubular sterilizer without a holding section.

$$\rho\left(u\frac{\partial \nu}{\partial z}+\nu\frac{\partial \nu}{\partial r}\right)=\frac{1}{r}\frac{\partial}{\partial r}(r\sigma_{rr})+\frac{\partial \sigma_{rz}}{\partial z} \quad (7)$$

where the stress components are:

$$\sigma_{rz}=\eta\left(\frac{\partial u}{\partial r}+\frac{\partial \nu}{\partial z}\right),\ \sigma_{zz}=-P+2\eta\frac{\partial u}{\partial z},$$
$$\text{and } \sigma_{rr}=-P+2\eta\frac{\partial \nu}{\partial r} \quad (8)$$

- energy equation

$$\rho c_p\left(u\frac{\partial T}{\partial z}+\nu\frac{\partial T}{\partial r}\right)=k\left[\frac{1}{r}\frac{\partial}{\partial r}\left(r\frac{\partial T}{\partial r}\right)+\frac{\partial^2 T}{\partial z^2}\right] \quad (9)$$

The boundary conditions for the equations are:

at $z=0$ and $0<r<R$,

$$u=u_{avg}\left(\frac{3n+1}{n+1}\right)\left[1-\left(\frac{r}{R}\right)^{(n+1)/n}\right],$$
$$\nu=0,\ \text{and}\ T=T_0;$$

at $z\geq 0$ and $r=R$, $u=0$, $\nu=0$, and $T=T_W$,

and at $z\geq 0$ and $r=0$, $\nu=0$

Physical Properties of the Fluid

Based on experimental rheological data, a TR model of 4% waxy rice starch dispersion applicable to thermal processing was obtained using the procedure described by Yang and Rao[10]. A set of experimental curves from temperature sweeps at several frequencies were superposed, and the complex and apparent viscosities were related using a modified Cox-Merz rule:

$$\eta_a=\left[C'\eta^*(T)\left(\frac{\omega_r}{\omega}\right)^{\beta}\right]^{\alpha'} \quad (10)$$

The TR model obtained (see Figure 2) was applied to the fluid flowing in the heating section where irreversible starch gelatinization took place. Because there was no other phase transition after gelatinization, the power law rheological equation combined with the Arrhenius equation were used

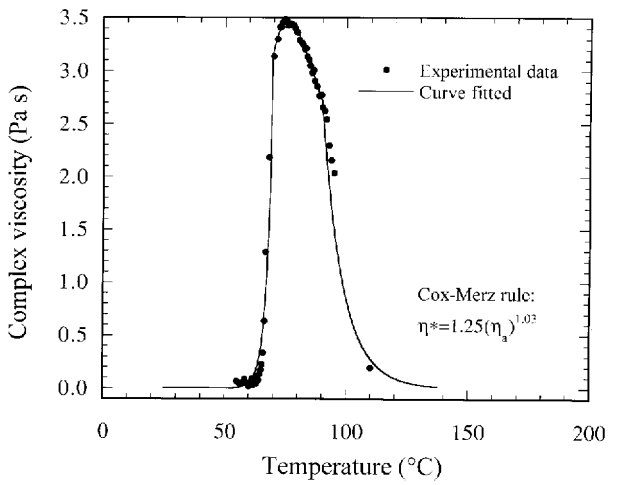

Figure 2. Thermo-rheological model during heating of starch dispersion used in the simulation.

Table 1. Power law parameters of gelatinized 4% waxy rice starch paste at different temperatures for simulation of cooling process.

Temperature (°C)	Consistency coefficient (K)	Flow behaviour index (n)	R^2
27	5.96	0.40	0.99
53	1.50	0.44	0.98
65	1.36	0.45	0.98
85	1.15	0.47	0.99
110	0.40	0.30	0.93

to describe the effect of shear rate and temperature of the gelatinized starch dispersion in the cooling section (see Table 1):

$$\eta_a=\eta_\infty\exp\left(\frac{E_a}{RT}\right)\left(\frac{\partial u}{\partial r}\right)^{n-1} \quad (11)$$

Before gelatinization, the starch dispersion was assumed to exhibit Newtonian behaviour, like water (the viscosity of water is 0.001 Pa s at 20°C) because of its high water content. Detailed description of the development of TR model of rice STD over the temperature range: 25–115°C can be found in Liao *et al.*[11]. These results were extrapolated and used in the present study conducted at the two heating section wall temperatures: 139°C and 145°C. As gelatinization of starch is completed by about 100°C, change in the apparent viscosity of the starch dispersion at temperatures > 100°C can be accounted by only temperature. Therefore, extrapolation of the experimental TR data to temperatures > 115°C should contribute to minimal errors. Another consideration was that it was not possible to obtain TR data above 115°C[11].

The changes in the other physical properties with temperature were neglected since they were not significant compared to the drastic changes in viscosity with temperature during gelatinization. The density, 971.8 kg m^{-3}, specific heat, 4199 J kg^{-1} K^{-1}, and thermal conductivity, 0.668 W m^{-1} K^{-1}, were assumed to be constant and to be the same as those of water at 80°C[12]. The various experimental variables studied are summarized in Table 2.

Lethality and Nutrient Retention

The rate of destruction of microbial spores is generally described by first order kinetics, expressed by the differential equation:

$$-\frac{dc}{dt}=k_T c \quad (12)$$

Table 2. Tube diameter, flow rate, heating wall temperatures, and kinetic parameters used in simulation.

Parameter	Value
Diameter of the tube	0.018 and 0.024 m
Flow rate	1.0 and 1.5 L min^{-1}
Heating wall temperature	139 and 145°C
Density	971.83 kg m^{-3}
Thermal conductivity	0.668 W m^{-1} K^{-1}
Specific heat	4199 J kg^{-1} K^{-1}
D- and z-values for *Cl botulinum*	$D_{121\cdot C}=0.27$ min, $z'=10$°C
D- and z-values for thiamine	$D_{121\cdot C}=158$ min, $z'=35$°C

The temperature dependency of rate constant is given by the well-known Arrhenius equation:

$$k_T = k_0 e^{-\frac{E_a}{RT}} \tag{13}$$

To obtain the final concentration under non-isothermal conditions, equation (13) is integrated between initial concentration c_i and concentration c at time t to get:

$$\ln\frac{c_i}{c} = k_0 \int_0^t e^{-\frac{E_a}{RT}}\,dt \tag{14}$$

Instead of referring to a final concentration, an equivalent heating time of F_0 is used that gives the same final concentration at reference temperature T_R as the given process at its temperature T. For a reference temperature of T_R, and a rate constant k_{T_R},

$$\ln\frac{c_i}{c} = \int_0^{F_0} k_{T_R}\,dt = \int_0^{F_0} k_0\left[e^{-\frac{E_a}{RT_R}}\right]dt = k_0\left[e^{-\frac{E_a}{RT_R}}\right]F_0 \tag{15}$$

Equating equation (14) and (15), the following expression is determined:

$$F_0 = \frac{k_0\int_0^t e^{-\frac{E_a}{RT}}\,dt}{k_0 e^{-\frac{E_a}{RT_R}} = \int_0^t e^{\frac{E_a}{R}\left(\frac{1}{T_R}-\frac{1}{T}\right)}\,dt} \tag{16}$$

When T is close to T_R, equation (16) can be simplified to:

$$F_0 = \int_0^t 10^{\frac{T-T_R}{z'}}dt \tag{17}$$

where, $z' = \dfrac{2.303RT_R^2}{E_a}$ is the z-value. The symbol z' is being used here for z-value to avoid conflict in nomenclature with the axial coordinate z.

Equation (17) provides the equivalent heating time F_0 at a reference temperature T_R for a process whose actual temperature T varies with time t. For the non-isothermal case of continuous tube flow, F_0 can be written by modifying equation (17) to:

$$F_0(L,r) = \int_0^L \frac{10^{\frac{T-T_R}{z'}}}{\frac{dz}{dt}}dz = \int_0^L \frac{10^{\frac{T(z,r)-T_R}{z'}}}{u(z,r)}\,dz \tag{18}$$

This equation assumes that spores of microbial organisms which remain do not move on their own and are simply carried by the fluid. The accumulated lethality value at the SHZ, instead of the average value, is of interest for food safety.

The concentration values at a certain spatial location in the tube can be written in terms of F_0 from equation (15) as:

$$\frac{c}{c_I} = e^{-k_{T_R}F_0} \tag{19}$$

For the nutrients, an average concentration which provides a measure of the nutritional quality of the processed food can be calculated by converting F_0 to nutrient content (equation (19)) and then determining the mean or 'mixing cup' nutrient content[1,5,13] at a given axial location:

$$c(z) = \frac{\int_0^R c(z,r)u(z,r)2\pi r\,dr}{\int_0^R u(z,r)2\pi r\,dr} \tag{20}$$

Thiamine was chosen as the component in the evaluation of nutrient retention in this study with z' 35°C and $D_{121°C}$ value 158 min[14].

Numerical Solution

The non-Newtonian behaviour and the temperature dependent viscosity made it very difficult to derive an analytical solution to the coupled governing momentum and energy transport equations. Therefore, a commercial Computational Fluid Dynamics package (FIDAP Version 7.6, Fluid Dynamics International, Evanston, IL) based on the finite element method was used to solve the governing continuity, momentum and heat transport equations on a personal computer platform (DELL, Intel Pentium II microprocessor, Windows NT operating system, 128 MB RAM, Round Rock, Texas). Description of FIDAP can be found in Engelman (1993) and of computer-aided food process engineering in Datta[15].

User subroutines of the non-Newtonian viscosity model of the starch-containing fluid and the boundary condition at the entrance of the heating section with fully developed velocity profile were written in FORTRAN and linked to the main code of FIDAP. When the computed shear rate was lower than 2.73 s^{-1}, the value of viscosity was assumed to be that at 2.73 s^{-1} to avoid infinite viscosity values.

In order to predict lethality accumulated at SHZ and average nutrient retention, a user-defined scalar variable routine describing the calculation was written in FORTRAN and linked to the FIDAP postprocessor. This subroutine used the temperature and velocity values at each nodal point obtained from solving the governing partial differential equations and performed the postprocessing to obtain the expected variables. The various integrals were evaluated using the simple trapezoidal rule.

A finite element (FE) mesh was defined with more nodes near the tube wall and the entrance of the tubular heat exchanger to resolve the large variations in temperature and velocities near the wall and the tube entrance. A total of 31 nodal points in the radial direction were used. The distance between the two nodal points next to the wall was six times smaller than the distance between the two nodal points near the centreline. The nodal points in between were established using the geometric ratio factor required to fit the specified numbers of 31 nodes. The FE mesh used in the axial direction had 150 nodes in the first two metres of the heating section with the distance between the last two nodal point being 0.02 m; again, the nodal points in between were established using the geometric ratio factor required to fit the specific number of nodes. In the rest of the heating section and the cooling section, the spacing between two nodal points was 0.02 m; as stated earlier, the length of the heating section was terminated when the accumulated lethality value on the centreline reached 5.0 min. Nine node quadrilateral elements were used. The dimensionless temperature vs dimensionless axial length profiles with spacing between nodal points of 0.01 m and 0.02 m were nearly identical (not shown here) so that the use of 0.02 m spacing was considered to be satisfactory.

For the purpose of comparison of mesh size, it is noted that Kumar and Bhattacharya[5] employed axial distances 0.025 and 0.01 m between two nodes, which gave the same results, and 25 nodes in the radial direction (radii of

the tubes employed were 6.35 and 9.53 mm). Bhamidipati and Singh[16] found that a radial grid spacing with 31 nodes gave good results for their study (radii of the tubes employed were 2.55 cm and 3.82 cm).

Solution scheme

The successive substitution iteration scheme was used to solve the partial differential equations that arose in a steady state analysis. The Stokes problem that is the linear problem associated with that to be simulated was first solved and provided a suitable initial guess to solve the nonlinear system of equations of the iterative procedure. The penalty function approach in which the continuity requirement is weakened was chosen; the value of the penalty parameter used in this simulation was 10^{-12}. The streamline upwinding option was added to control the solution vector oscillations primarily caused by advection terms in the Galerkin finite element formulation[17]. Iteration for the steady-state solution was terminated when the following two convergence criteria were satisfied simultaneously:

$$\left\| \frac{u_i - u_{i-1}}{u_i} \right\| \leq 0.005 \tag{21}$$

and

$$\left\| \frac{R_i}{R_0} \right\| \leq 0.005 \tag{22}$$

where u is the solution vector and R the residual force vector. The norm $\|\cdot\|$ is a root mean square norm summed over all the nodes in the mesh.

RESULTS AND DISCUSSION

Verification of Numerical Technique

One technique for verification of a numerical model is by solving a simpler problem with either a known or an easy to verify solution[16]. In this study, the results of simulation of laminar isothermal flow of a power law fluid ($n = 0.5$) were compared with those reported by Lyche and Bird[2]. The same assumptions as those made by Lyche and Bird[2] were employed for the numerical verification: negligible axial heat conduction, power law fluid with all other physical properties constant, steady state flow, and no viscous dissipation. Figure 3 shows that the numerical results obtained using FIDAP were in good agreement with those of Lyche and Bird[2].

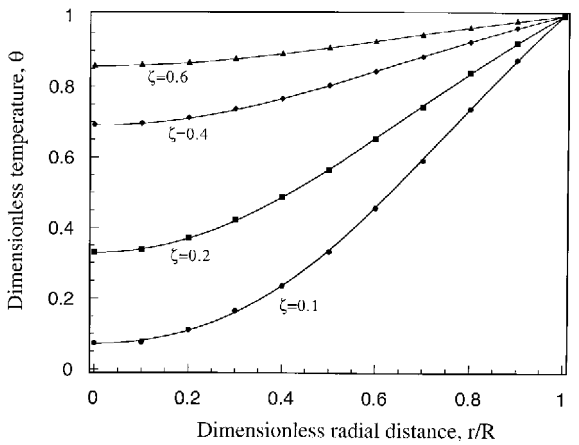

Figure 3. Comparison of heat transfer simulation results for laminar isothermal flow of power law fluid, $n = 0.5$; filled symbols are results from Lyche and Bird[2] and solid lines are simulation results.

Analysis of the Heating Section

At the entrance of the heat exchanger, a fully developed parabolic flow profile boundary condition was assumed with the maximum velocity on the centreline being twice the average velocity. As the starch dispersion flowed in the heating section, the fluid near the wall was first heated. Such radial temperature gradient caused the thermally induced starch gelatinization to begin near the wall and move toward the centreline downstream of the tube. The resulting radial viscosity gradient thus distorted the flow profiles considerably. Figure 4 shows the centreline velocities and tempera-

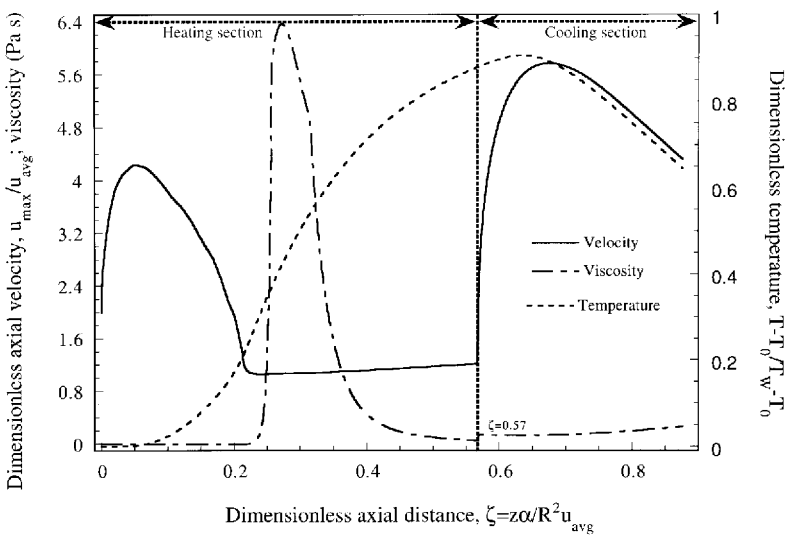

Figure 4. Dimensionless axial velocity and temperature near the centreline along the length of the tube; $R = 0.012$ m, $T_w = 145$°C; $Q = 1.0$ L min^{-1}. Note the sharp increase in velocity at the beginning of heating and cooling sections.

tures in dimensionless form along the length of the tube. Figures 5 and 6 contain the dimensionless velocity profiles at different axial and radial locations in the heating and cooling sections, respectively.

Figures 7 and 8 show the dimensionless temperature profiles at different locations along the length of the tube. As can be seen in Figure 7, the temperature across the cross section became more uniform as the fluid flowed further into the heating section as well as in the cooling section. At the entrance of the heating section, the flow profile was distorted into two distinguishable parts across the cross section; a plateau occurred in the flow profile for the fluid travelling away from the centreline and the rest of the flow across the cross section was significantly distorted.

Limiting cases have been solved theoretically for the velocity profiles of non-isothermal laminar tube flow by Kwant *et al.*[18,19]. Simpson and Williams[1] pointed out that the blunting effect caused by the shear-thinning nature of the fluid increased the total probability of sterility by nearly twenty orders of magnitude in comparison to the incorrect assumption that the food was Newtonian. With the more accurate velocity profiles obtained, the safety parameters (i.e. cumulative lethality and mean nutrient retention) may

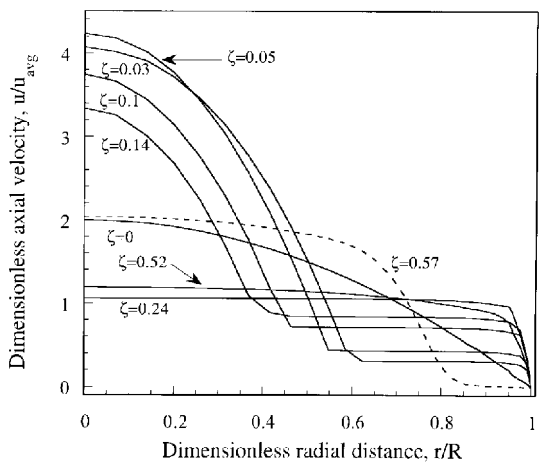

Figure 5. Radial dimensionless velocity profiles at different distances from entrance in heating section, $R = 0.012$ m; $T_w = 145$°C; $Q = 1.0$ L min^{-1}. Note that the velocity profiles became flat at $\zeta = 0.24 - 0.57$.

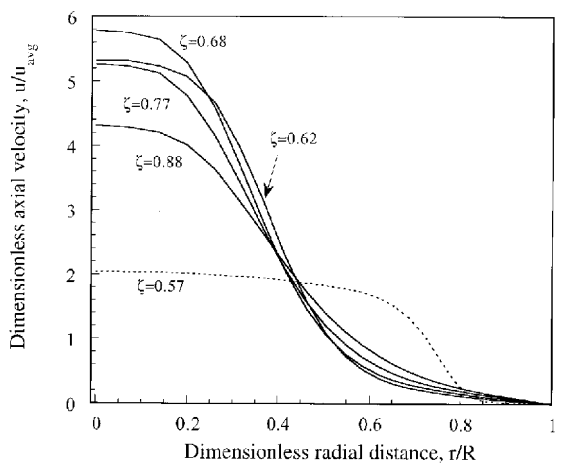

Figure 6. Radial dimensionless velocity profiles at different distances from entrance in cooling section, $R = 0.012$ m; $T_w = 145$°C; $Q = 1.0$ L min^{-1}.

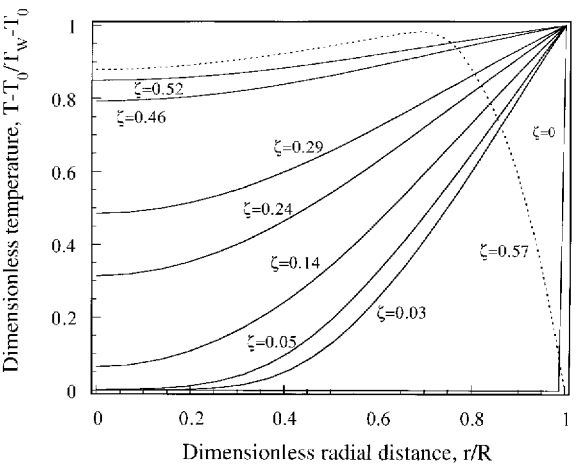

Figure 7. Radial dimensionless temperature profiles at different distances from entrance in heating section, $R = 0.012$ m; $T_w = 145$°C; $Q = 1.0$ L min^{-1}. The temperature became uniform with increase in length (ζ).

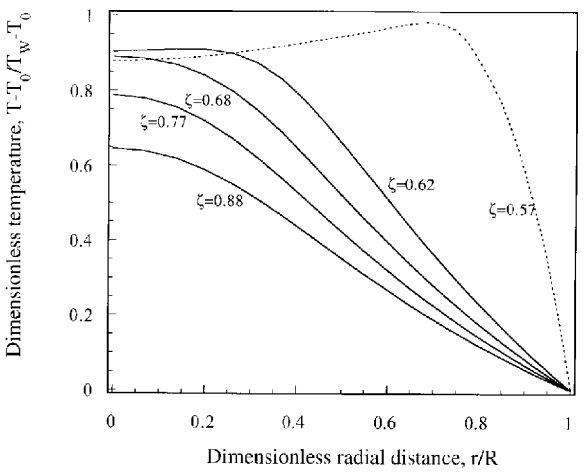

Figure 8. Radial dimensionless temperature profiles at different distances from entrance in the cooling section, $R = 0.012$ m; $T_w = 145$°C; $Q = 1$ L min^{-1}.

be incorporated as requirements for optimal design. The occurrence of the plug-flow profile led to a decrease in centreline velocity, which in turn affected the product lethality.

As shown in Figure 5 and as expected, at the beginning of the heating section, the maximum velocity was always on the centreline and was higher than the average velocity by as much as 4.2 times the average value. However, as the fluid continued travelling along the tube, the centreline velocity decreased to almost the same magnitude as the average velocity. The profile became much flatter and tended towards plug-flow. The portion of the flow blunted was related to the TR behaviour caused by gelatinization of starch and the bluntness increased as the fluid travelled further in the heating section. As the temperature on the centreline reached the initial temperature of starch gelatinization of about 62°C, the viscosity of the fluid on the centreline began to be strongly dependent on temperature, resulting in plug-flow profile being completely developed at the axial location $\zeta = 0.24$. At this location, the starch-containing fluid travelling along the centreline began to gelatinize.

In Figure 9, it can be seen that the velocity profiles were distorted because of the radial viscosity gradients: (1) at $\zeta = 0.05$, the plateau in the velocity profile was related to the fluid undergoing gelatinization, (2) at $\zeta = 0.24$, the velocity profile tended to be that of plug-flow and the fluid elements across the entire cross section were undergoing gelatinization, and (3) at $\zeta = 0.29$, the plug-flow profile still remained. Figure 10 shows the profiles of temperature, viscosity, shear rate, and dimensionless velocity across the radial cross section at $\zeta = 0.11$. The velocity profile was significantly distorted with a plateau between $r/R = 0.45$ and 0.95. In addition, while the effect of shear rate on the viscosity of the fluid flowing in the tube was not so significant, it seems that starch gelatinization which began at about 62°C caused the plateau in the velocity profile leading to very low shear rates.

Further along the heating section, the temperature became more uniform across the cross section and the centreline velocity started to increase slightly. Simpson and Williams[1] and Kumar and Bhattacharya[5] found that the flow profile at the end of the heating section reverted to the isothermal flow profile at the entrance of heating section. But this was not the case here since thermo-rheological properties of the starch dispersion still played a major role at the end of the heating section.

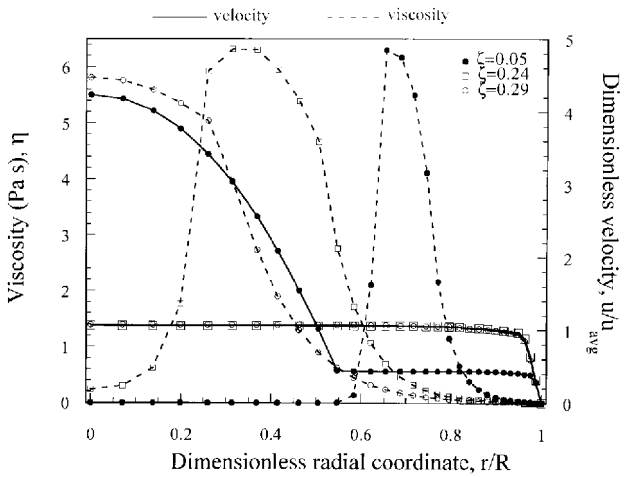

Figure 9. Radial velocity and viscosity distribution at different distances from the entrance ($\zeta = 0.05,\ 0.24,\ 0.29$), $R = 0.012$ m; $T_w = 145$°C; $Q = 1.0$ L min^{-1}. Note the plug-flow profile over most of the tube's cross section at $\zeta = 0.24$ and 0.29.

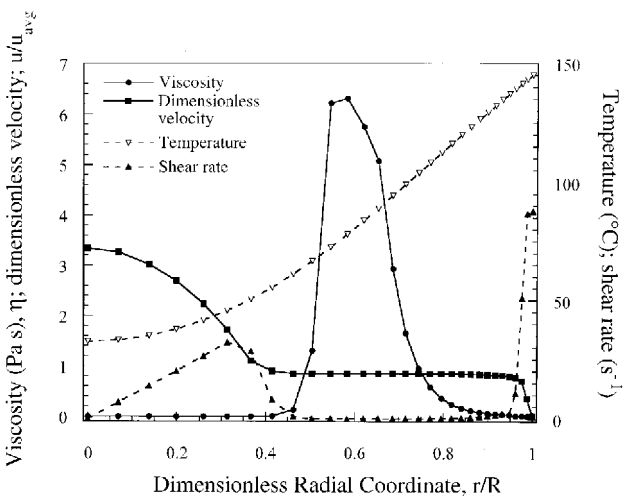

Figure 10. Radial temperature, shear rate, viscosity, and dimensionless velocity profiles in the heating section at $\zeta = 0.11$; $R = 0.012$ m; $T_w = 145$°C; $Q = 1.0$ L min^{-1}. Starch gelatinization which began at about 62°C caused the plateau in the velocity profile.

Analysis of Cooling Section

When the heated fluid entered the cooling section, the temperature of the fluid travelling near the tube wall dropped rapidly causing the viscosity of the fluid to increase. Again, this spatial variation in viscosity forced the fluid travelling away from the wall to move faster (also observed by Simpson and Williams[1] and Kumar and Bhattacharya[5]) and thus the maximum centreline velocity was approximately 5.8 times the average value (see Figure 6). The temperature on the centreline continued to increase in the initial part of the cooling section and the temperatures were high enough for sterilization to be still effective. The additional lethality gained in the cooling section could contribute towards additional lethality that makes the design more conservative.

Length of Heating Section

Effect of wall temperature

Simpson and Williams[1] suggested a dimensionless length heating section ($\zeta_H = z_H \alpha / R^2 u_{avg}$) of 0.8 for shear-thinning fluids with or without temperature dependence; they assumed that the heating section was terminated when the temperature gain on the centreline was 95% and an F_0 of 2.45 min was assured. In this study, an accumulated F_0 of 5 min on the centreline was specified before the fluid exited the heating section. As the fluid achieved the same sterility at the end of heating section, the actual length of the heating section varied with the design parameters: flow rate, heating wall temperature, and diameter of the tube.

The dimensionless length of the heating section was about 0.56–0.60 when the heating wall temperature was 145°C (see Table 3). Decreasing the tube wall temperature (139°C) resulted in an increase in the dimensionless heating section length to $\zeta_H = 0.67$. At the heating wall temperature 145°C, the effective contribution to food lethality started earlier in the tube so that a shorter length was required to achieve sterility (see Figure 11).

Effect of flow rate

In contrast to heating wall temperature, increasing the flow rate resulted in an increase in the actual length of heating section (other parameters being held constant) because of the change in the residence time required in the tube to achieve the sterility. Increasing the flow rate by 50% caused a 50% increase in the actual length of heating section but, as can be seen in Figure 12, the average thiamine retention remained unchanged. Decreasing the heating wall temperature produced higher nutrient retention along the tube but the final nutrient content at the end of the heating section was almost unchanged because a longer length of tube was needed to achieve sterility. Increasing the tube diameter resulted in more destruction of nutrient. Table 4 shows the temperature and velocity data in all the cases.

Table 3. Dimensionless length of heating section, accumulated lethality and thiamine retained at the end of heating section for different tubes, wall temperatures, and flow rates.

Tube Diameter (m)	Wall temperature (°C)	Flow rate (L min^{-1})	u_{avg} (m s^{-1})	ζ_H	Lethality (min)	Thiamine (c/c_I)
0.018	139	1.0	0.066	0.67	5.04	0.905
0.018	139	1.5	0.098	0.67	5.45	0.907
0.018	145	1.0	0.066	0.59	5.49	0.904
0.018	145	1.5	0.098	0.60	6.50	0.902
0.024	139	1.0	0.037	0.67	5.53	0.842
0.024	139	1.5	0.055	0.67	7.40	0.844
0.024	145	1.0	0.037	0.57	5.01	0.837
0.024	145	1.5	0.055	0.56	5.33	0.848

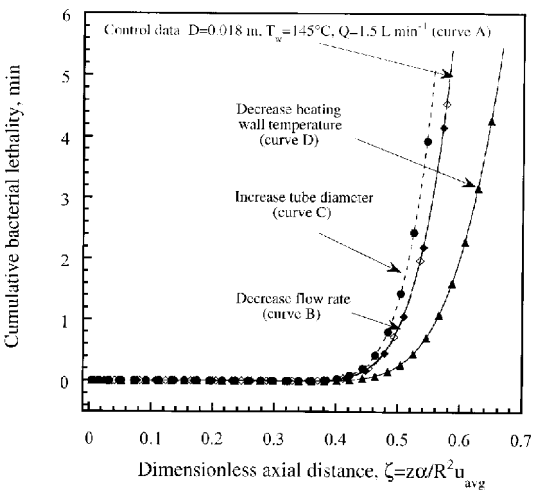

Figure 11. Cumulative lethality on the centreline along the heating section for two flow rates: 1.5 and 1.0 L min^{-1} (B), heating wall temperature: 139 (D) and 145°C, and tube diameters: 0.018 and 0.024 m (C). Note that the lethality was close to zero until $\zeta = 0.45$ and increased rapidly for higher value of ζ.

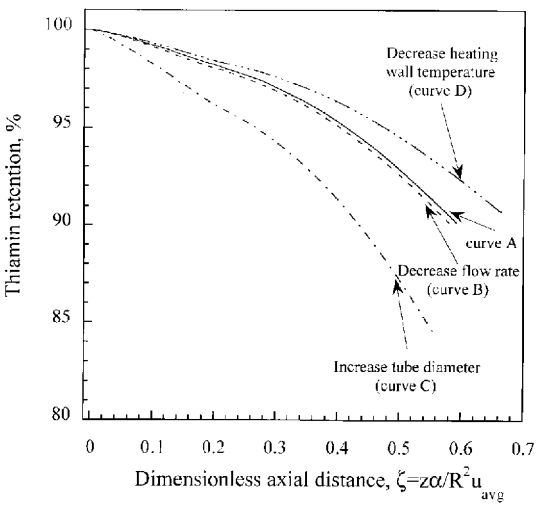

Figure 12. Thiamine retention along the length of the heating section for two flow rates: 1.5 and 1.0 L min^{-1} (B), heating wall temperature: 139 (D) and 145°C, and tube diameters: 0.018 and 0.024 m(C). Curve A: D = 0.018 m, T_w = 145°C, Q = 1.5 L min^{-1}.

The minimum centreline velocity was close to average velocity leading to the plug-flow in the tube in all the cases.

Role of rheological behaviour

Sterilization of different fluid foods, to achieve the same 5.0 min of lethality value at the SHZ, with different rheological behavior required different heating tube lengths with $R = 0.009$ m; $T_w = 139$°C; $Q = 1.5$ L min^{-1}. The dimensionless heating lengths required were[20]: (1) 0.69 to sterilize a fluid that obeyed the temperature dependent power law model (equation (11)) when there was no effect of starch gelatinization on sterilization in the heating tube, (2) 0.85 to sterilize a Newtonian fluid, and (3) 0.67 to sterilize a starch-containing fluid (equation (10)) because of the occurrence of the plug-flow profile in the heating tube.

Table 4. Maximum centreline velocities in heating and cooling sections, and minimum velocities in the heating section, as well as the corresponding values of the dimensionless axial distance (ζ) and temperature (θ).

			Heating section						Cooling section	
			Maximum velocity			Minimum velocity			Maximum velocity	
Tube Dia (m)	Wall temp (°C)	Flow rate (L min^{-1})	u_{max}/u_{avg}	ζ ($\times 10^2$)	θ ($\times 10^3$)	u_{min}/u_{avg}	ζ	θ	u_{max}/u_{avg}	θ
0.018	139	1.0	3.87	5.34	2.93	1.06	0.242	0.330	6.11	0.928
0.018	139	1.5	3.51	5.23	2.54	1.07	0.230	0.320	6.27	0.932
0.018	145	1.0	3.38	4.34	1.20	1.08	0.219	0.312	6.34	0.906
0.018	145	1.5	3.09	4.48	1.29	1.10	0.211	0.304	6.47	0.911
0.024	139	1.0	5.40	5.46	3.17	1.05	0.273	0.336	5.64	0.917
0.024	139	1.5	4.52	5.68	3.32	1.05	0.259	0.336	5.95	0.924
0.024	145	1.0	4.24	5.11	1.77	1.06	0.241	0.313	5.77	0.892
0.024	145	1.5	3.71	5.35	2.63	1.07	0.227	0.308	6.08	0.894

CONCLUSIONS

Accurate thermo-rheological behaviour of food is important for optimizing thermal process design in a tubular sterilizer. The plug-flow profile that occurred in the heating section was caused by gelatinization of the starch-containing fluid food. Without compromising the sterility for starch-containing fluid food flowing in the tubular sterilizer, smaller diameter tubes lead to better nutrient quality (higher thiamine retention). Nutrient retention did not change appreciably with lower heating wall temperature or volumetric flow rate. Higher volumetric flow rate resulted in a longer length of heating section to achieve the sterility of the product but the thiamine retention was almost unchanged. Thus the diameter of the tube is the most important design parameter when considering nutrient retention and similar first-order quality changes for sterilization of starch-containing fluid foods.

NOMENCLATURE

C	constant, $C' = C^{-1}$
c	concentration of bacterial spores or a nutrient
c_i	initial concentration of bacterial spores or a nutrient
c_P	specific heat, J kg^{-1} K^{-1}
D	decimal reduction time, min
E_a	activation energy, J mol^{-1}
F_0	equivalent processing time at reference temperature, min
k	thermal conductivity, J m^{-1} K^{-1} s^{-1}
K, K_0	consistency index, Pa s^n
k_T	rate constant at temperature T
k_{T_R}	rate constant at reference temperature T_R
L	length, m
n	flow behaviour index
Q	volumetric flow rate, L min^{-1}
R	gas constant, 8.314 J mol^{-1} K^{-1}); tube radius (m); residual force vector
r	radial coordinate, m
T	temperature, °C or K
t	time, sec
T_0	initial temperature of the fluid, °C or K
T_R	reference temperature, °C or K
T_w	wall temperature, °C or K
u	axial velocity, m s^{-1}
u_{avg}	average velocity, m s^{-1}
V	total volume of the liquid, m^3
v	radial velocity, m s^{-1}
z	axial coordinate, m
z'	$z-\text{value} = \dfrac{2.303RT_R^2}{E_a}$

Greek letters

α	constant, $\alpha' = \alpha^{-1}$; thermal diffusivity$= k/\rho c_p$
β	shift factor
$\dot{\gamma}$	shear rate, s^{-1}
ε_f	residual tolerance parameter
ε_u	velocity convergence parameter
η^*	complex viscosity, Pa s
η_a	apparent viscosity, Pa s
η_∞	viscosity at infinite temperature, Pa s
η_R^*	reduced complex viscosity
ρ	density, kg m^{-3}
σ	stress, Pa
ω	frequency, rad s^{-1}
ω_r	reference frequency, rad s^{-1}
ψ	$= \left(\dfrac{E_a}{R}\right)\left(\dfrac{1}{T_0}-\dfrac{1}{T_w}\right)$
ζ	reduced axial dimension $= z\alpha/R^2u_{avg}$
ζ_H	reduced length of heating section

REFERENCES

1. Simpson, S.G. and Williams, M.C., 1974, An analysis of high temperature/short time sterilization during laminar flow, *J Food Sci*, 39: 1047–1054.
2. Lyche, B.C. and Bird, R.B., 1956, The Graetz-Nusselt problem for a power-law non-Newtonian fluid, *Chem Eng Sci*, 6: 35–41.
3. Wissler, E.H. and Schechter, R.S., 1959, The Graetz-Nusselt problem with extension for a Bingham plastic, *Chem Eng Prog Symp Ser*, 29–34.
4. Christiansen, E.B. and Craig, S.E, 1962, Heat transfer to pseudoplastic fluids in laminar flow. *AIChE J*, 8: 154–160.
5. Kumar, A. and Bhattacharya, M., 1991, Numerical analysis of aseptic processing of a non-Newtonian liquid food in a tubular heat exchanger, *Chem Eng Comm*, 103: 27–51.
6. Jung, A. and Fryer, P.J., 1999, Optimising the quality of safe food: Computational modeling of a continuous sterilisation process, *Chemical Eng Sci*, 54: 717–730.
7. Yang, W. H. and Rao, M. A., 1998, Numerical study of parameters affecting broken heating curve, *J Food Eng*, 37: 43–61.
8. Eliasson, A.C, 1986, Viscoelastic behavior during the gelatinization of starch, *J Texture Studies*, 17: 25265.
9. Okechukwu, P.E. and Rao, M.A., 1995, Influence of granule size on viscosity of cornstarch suspension, *J Texture Studies* 26: 501–516.
10. Yang, W.H. and Rao, M.A., 1998, Complex viscosity-temperature master curve of cornstarch dispersion during gelatinization, *J Food Proc. Eng*, 21: 191–207.
11. Liao, H-J., Tattiyakul, J. and Rao, M. A, 1999, Superposition of complex viscosity curves during gelatinization of starch dispersion and dough, *J Food Process Eng*, 22: 215–234.
12. Geankoplis, C.J., 1993, *Transport Processes and Unit Operations* (PTR Prentice-Hall, Inc, Englewood Cliffs, New Jersey).
13. Guariguata, C., Barreiro, J.A., and Guariguata, G., 1979, Analysis of continuous sterilization processes for Bingham plastic fluids in laminar flow, *J Food Sci*, 44: 905–910.
14. Feliciotti, E. and Esselen, W.B., 1957, Thermal destruction rates of thiamine in pureed meats and vegetables, *Food Technol*, 11: 77.
15. Datta, A. K., 1998, Computer-aided engineering in food process and product design, *Food Technol*, 52(10): 44–52.
16. Bhamidipati, S. and Singh, R.K, 1994, Thermal time distribution in tubular heat exchangers during aseptic processing of fluid foods, *Biotechnol Prog*, 10: 230–236.
17. Brooks, A.N. and Hughes, T.J.R, 1982, Streamline upwind/Petrov-Galerkin formulations for convection dominated flows with particular emphasis on the incompressible Navier-Stokes equations, *Comp Methods Appl Mechanics and Eng*, 32: 199–259.
18. Kwant, P.B., Fierens, R.H.E. and Van Der Lee, A, 1973, Non-isothermal laminar pipe flow – I. Theoretical, *Chemical Eng Sci*, 28: 301–316.
19. Kwant, P.B., Zwaneveld, A. and Dijkstra, F.C., 1973, Non-isothermal laminar pipe flow – II Experimental, *Chemical Eng Sci*, 28: 1317–1330.
20. Liao, H-J., 1998, Simulation of continuous sterilization of fluid food products: the role of thermorheological behavior of starch dispersion and process optimization, *PhD thesis* (Cornell University, Ithaca, NY).

ACKNOWLEDGEMENTS

We are grateful to the USDA for a NRI Grant #97-35503-4493, the California Natural Products, Lathrop, CA, for donation of starch samples, and to Intel Corporation for providing the Dell personal computer platform.

ADDRESS

Correspondence concerning this paper should be addressed to Dr M.A. Rao, Department of Food Science and Technology, Cornell University, Geneva, NY 14456-0462, USA. E-mail: mar2@cornell.edu.

The manuscript was received 17 June 1999 and accepted for publication after revision 21 January 2000.